

## Textural Characteristics, Mode of Transportation and Depositional Environments of the Southern Bredasdorp Basin, as Revealed from Lithofacies and Grain Size Analyses

*Temitope Love Baiyegunhi, Oswald Gwavava and Kuiwu Liu*

*Department of Geology, Faculty of Science and Agriculture, University of Fort Hare, South Africa*

Received November 26, 2022; Accepted May 26, 2023

---

### **Abstract**

The Bredasdorp Basin comprises the majority of the larger Outeniqua Basin, which is a productive petroleum-bearing basin off South Africa's south coast. Despite the basin's distinct stratigraphic sequence and lithological variation, there are few sedimentological details about the lithofacies characteristics and grain size parameters. As a result, the mode of transport, hydrodynamic energy conditions, and depositional environment are poorly documented. Grain size and lithofacies studies on preserved cores from five exploration wells in the basin were performed to unravel their textural characteristics, hydrodynamic energy conditions, depositional processes and depositional environments. These cores are from the 6At1 and 14At1 stratigraphic sequences' primary and secondary hydrocarbon targeted intervals. The statistical parameters of grain-size distribution (mean grain size, standard deviation, skewness, and kurtosis) indicate that the sandstones are primarily unimodal, fine-grained, moderately well sorted, mesokurtic, and near-symmetrical. The bivariate diagrams of the statistical parameters mentioned above show that the impact of wave and river processes on depositional environments was the greatest. The linear discriminant functions (LDF) analysis shows that the sandstones are turbidity current deposits under coastal dune and beach process in a shallow marine environment. Similarly, the C-M pattern (Passega diagram) indicates that the sandstones were deposited primarily by a tractive current process (beach/tidal). The log-probability weight plots suggest that the hydraulic depositional conditions are erratic (variable). Saltation is the primary mode of transportation, followed by suspension and traction. Thirteen sedimentary lithofacies were identified and classified into six lithofacies associations (FA1-FA6). These lithofacies associations FA1, FA2, FA3, FA4, FA5 and FA6 are interpreted as submarine channel-fills, submarine channel-levee, submarine sheet lobe, submarine lobe fringe/overflow, basin plain deposits, and deep-sea floor/basin plain deposits, in that order.

**Keywords:** Grain-size; Texture, Lithofacies; Hydrodynamic energy condition; Bredasdorp Basin.

---

## **1. Introduction**

Sedimentary facies is a type of sedimentary rock that has specific compositional, petrological, and sedimentary characteristics that indicate the depositional conditions that existed prior to or during the formation of the rock. Furthermore, sedimentary facies is any restricted part of a designated stratigraphic unit that exhibits characteristics that differ significantly from other parts of the unit [1]. A sedimentary facies' descriptive aspect includes the identification and documentation of characteristics or features such as colour, texture, lithology, grain size, mineral compositions, fossil content, and sedimentary structures. Middleton [2] emphasized the importance of combining observations made on their spatial relations and internal characteristics such as sedimentary structures with comparative information from other well-studied stratigraphic units. Reading [3] and Miall [4] stated that in order to accurately interpret depositional environments, it is necessary to determine the relationship of facies to one another as well as identify facies that tend to occur together rather than analysing individual or isolated facies. According to Nyathi [5], close or neighbouring facies can represent nearby or

adjacent depositional environments, and the way these facies relate to one another is depicted in the facies characteristics. Sedimentary facies can be classified into facies associations, and the term "facies association" refers to a group of facies that occur together and are thought to be genetically or environmentally related [3,6]. Facies associations are frequently used to deduce the sedimentary process (es) that took place in the depositional environment. As a result of these processes, the depositional environment has distinct characteristics; thus, there is a link between the depositional environment and facies associations.

Similarly, grain size distribution is one of the most important properties of sediment particles because the size of grains in a particular deposit reveals hydrodynamic energy as well as transportation and depositional processes. Grain size analysis is a technique for determining grain size variations in lithified rock or loose deposit samples. Sediments are laid down in different environments and thus have varying particle sizes due to differences in erosional processes, transportation, and deposition histories. As a result, because it can reflect changes in water energy and depth in depositional environments, grain size analysis is an important tool for environmental reconstruction [7-9]. Some of the statistical parameters used to describe particle size distributions were depicted by Folk [10] and Folk and Ward [11]. Statistical parameters include mean grain size, sorting, skewness, and kurtosis.

These parameters can be displayed as histograms, cumulative frequency curves, or bivariate scatter plots. Many researchers have used bivariate scatter plots of statistical parameters to demarcate areas where deposits from specific environments can be plotted [12-15]. The grain size distribution, erosion processes, and transportation history of sediments determine their mean grain size, sorting, and skewness [16]. Flow regime fluctuations affect sediment supply and transport, while sediment mobilization changes channel morphology, according to [17]. Alternatively, several researchers, including Visher [18] and Sagoe and Visher [19] have used log-probability plots to deduce the hydrodynamic condition of sediments. This is due to the environmental significance of the shapes of grain size cumulative curves.

According to Visher [18], such curves typically have three or four straight-line segments rather than the single straight line expected for a normally distributed population. Visher [18] and Sagoe and Visher [19] infer that these straight-curve segments represent sub-populations of grains transported concurrently by dissimilar modes of transportation (i.e., traction, saltation and suspension). The differences in curve shape and the location of truncation points of curve segments allegedly allow demarcation or separation of sediments from different depositional environments. The southern Bredasdorp Basin stratigraphic sequence consists of sandstone, mudstone, and shale with subordinate siltstones. Despite the distinct stratigraphic sequence and lithological variation in the Bredasdorp Basin, few sedimentological details about the lithofacies characteristics and grain size parameters of the southern Bredasdorp Basin sandstones have been reported. To fill the void, lithofacies and grain size analyses were performed on five offshore exploration wells (boreholes E-AH1, E-AJ1, E-BA1, E-BB1, and E-D3) in the southern Bredasdorp Basin (Figure 1). The first detailed lithofacies and grain size analyses of selected rocks from the southern Bredasdorp Basin are presented in this study. The lithofacies characteristics, as well as the calculated statistical parameters and their interrelationships, linear discriminant function (LDF) analysis, Passega C-M diagram, and log-probability curves, are used to highlight various aspects of the transportation and depositional conditions that the sediment grains underwent, as well as to relate them to specific depositional environments. Furthermore, the lithofacies statistical analysis inferred depositional environments were compared for any discrepancies.

## 2. Geological setting

The Bredasdorp Basin is a rift basin with half-graben structures that runs south-east. These half-grabens are dominated by Upper Jurassic, Lower Cretaceous, Cretaceous, and Cenozoic rift to drift strata [21]. The basin formed as a result of rift and drift activity along the Agulhas-Falkland Fracture Zone during the breakup of the Gondwana supercontinent, along with other

sub-basins of the larger Outeniqua Basin (Figure 1) [22]. The Bredasdorp Basin, off South Africa's south coast (southeast of Cape Town and west-southwest of Port Elizabeth), is primarily composed of sandstones with subordinate mudrocks.

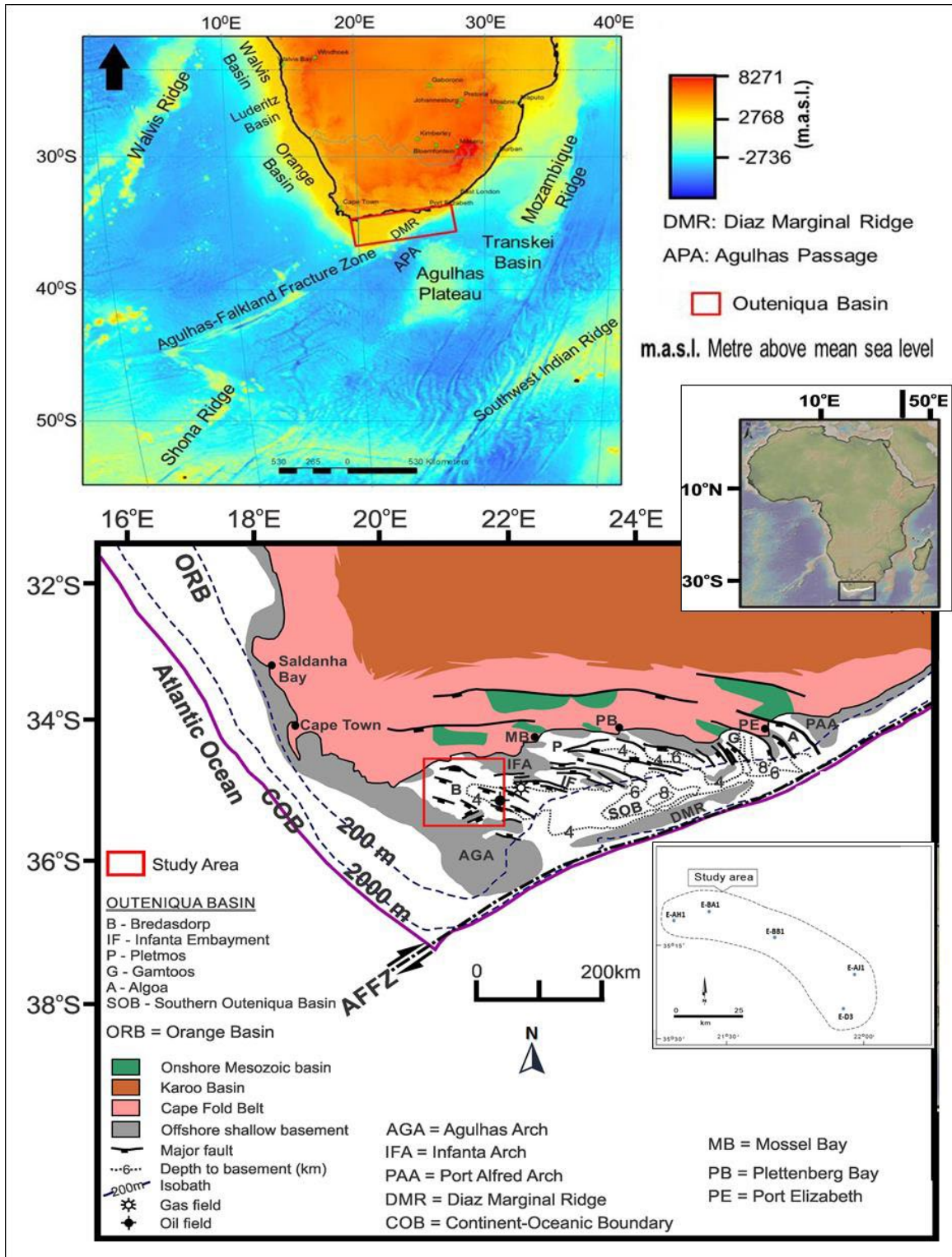


Figure 1. Geological map showing the studied exploration wells in Bredasdorp Basin as well as the distribution other Southern African offshore Basins [20]

The basin is approximately 80 km wide and 20 km long [23], with the Columbine-Agulhas Arch (CAA) and the Infanta Arch (IA) forming the western and eastern boundaries, respectively [21]. The CAA and IA are extended basement highs made up of Precambrian (basement) metamorphic rocks and Cape Supergroup granite. The Bredasdorp Basin is thought to have formed beneath the Indian Ocean along the South African continental margin during the early stages of rifting in the late Jurassic-early Cretaceous period [24]. According to Akinlua *et al.* [25], the basin underwent a series of structural distortions during the breakup of Gondwanaland and the southern hemisphere's continents. The Falkland-Agulhas Fracture Zone (AFFZ) produced dextral trans-tensional stress or right-lateral shear movement as a result of the separation of the Falkland Plateau from the Mozambique Ridge and the break-up of west Gondwana, according to Tinker *et al.* [26]. As a result of the tectonic events, normal faulting developed north of the AFFZ, resulting in the formation of graben and half-graben sub-basins (e.g., the Bredasdorp Basin) [21]. Late Jurassic and early Cretaceous syn-rift continental and marine sediments, as well as post-Cretaceous and Cenozoic divergent rocks with slanting or inclined half-graben structures, dominate the basin. The basin is formed by an Oxfordian-Recent stratigraphic column [21-22] that overlies the Cape Supergroup [27]. The stratigraphic column depicts the occurrence of a syn-rift phase and a post-rift or drift phase [28]. There are two sedimentation phases in the syn-rift phase: syn-rift I and syn-rift II [28]. The syn-rift I sedimentation occurred between the middle Jurassic and the late Valanginian (Basement to 1At1), while the syn-rift II sedimentation occurred between the late Valanginian and the Hauterivian (1At1 to 6At1) (Figure 2) [22].

The syn-rift I succession is terminated by a regional 1At1 unconformity, indicating the beginning of a renewed rifting (synrift II) phase caused by early movement along the AFFZ around 121 Ma (Valanginian-Hauterivian boundary) [28]. Later, during the Hauterivian-Early Aptian (6At1 to 13At1) period, the Transitional (Early Drift) phase occurred (Figure 2). The Transitional (Early Drift) phase was characterized by recurring episodes of progradation and aggradation and it was primarily influenced by tectonic events and eustatic sea-level changes [23]. This phase was considered the first deep water deposits in the Bredasdorp Basin, and they were deposited as a result of major subsidence of the basin as well as an increase in water depth. The late drift phase, on the other hand, coincided with a major marine regression in the Bredasdorp Basin during the early Aptian. This regression event caused significant erosion, which resulted in the 13At1 unconformity. Following the erosion period, a marine transgression transports and deposits organic-rich claystone in the basin under anoxic conditions [27]. When the Columbine-Agulhas Arch was cleared by the trailing edge of the Falkland Plateau in the Late Albian, the 14At1 mid-Albian unconformity (Figure 2) marked the start of active thermally driven subsidence [23].

### 3. Materials and methods

Sedimentological core logging was performed on the preserved cores from five exploration wells in the southern Bredasdorp Basin (E-AH1, E-AJ1, E-BA1, E-BB1, and ED3) (Figure 1; Table 1). These cores are interbedded sandstone and mudrock sequences that were cut from the primary and secondary hydrocarbon targeted intervals within the 6At1 and 14At1 stratigraphic sequences (Figure 2). The available cores from boreholes E-AH1, E-AJ1, E-BA1, E-BB1, and ED3 serve as the foundation for lithofacies analysis. The lithofacies analysis incorporates sedimentological data such as lithology, colour, grain size, mineral compositions, bedding characteristics, and sedimentary structures. For the facies analysis, a modified version of Miall's [4] lithofacies classification and coding was used. The lithofacies types identified were classified into facies associations (FAs), which were then used to interpret or deduce possible depositional palaeoenvironments. To cover textural variations, ninety-two representative thin sections of different sandstone types from the five exploration wells were selected systematically for grain size analysis (i.e., grain size, shape, and arrangement). The selected sandstones' grain size, textural parameters, and statistical relationships were investigated. The grain sizes were measured on thin sections using a petrographic microscope with a calibrated eyepiece. Using the traditional method of measuring the longest axis of the grain, a minimum

of 500 grains were measured per thin section. The grain size dimensions were then converted to normal sieve grain sizes as proposed by [29].

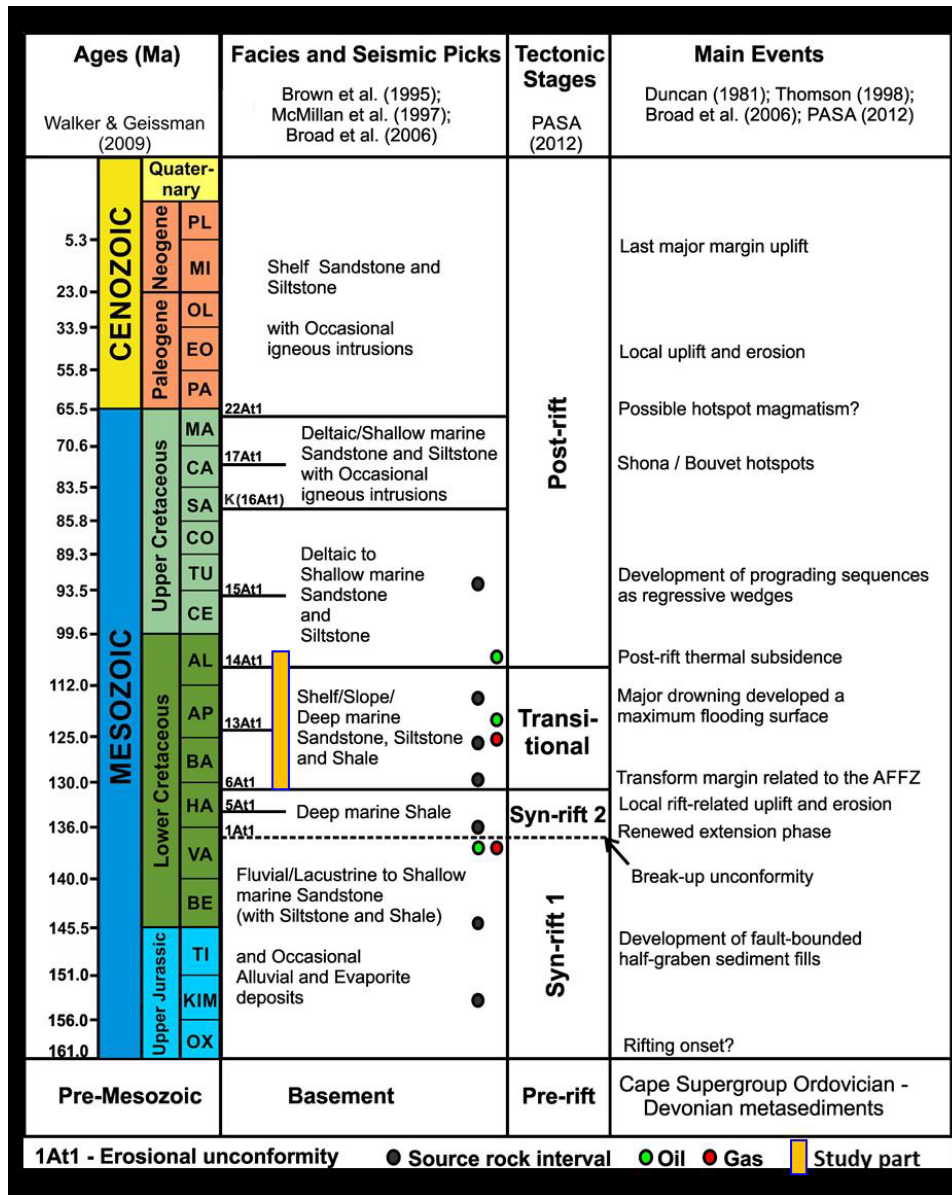


Figure 2. Stratigraphic chart of the Bredasdorp Basin showing main unconformities and tectonic stages with corresponding geodynamic events [20]

Because grains in sedimentary rocks have a wide range of size distributions, the frequencies of grain size ranges were calculated, and grain size classes were determined using the Udden-Wentworth grade scale [30]. Certain standard statistical measures for grain size distribution in clastic sedimentary rocks are typically described, and these can be further subdivided into four main parameters: graphic mean, graphic standard deviation, graphic skewness, and graphic kurtosis. Boggs [6] and Baiyegunhi and Liu [31] provide detailed information or definitions of the statistical parameters. These statistical parameters were calculated using the equations by [10]. Table 2 shows the statistical parameters and their verbal equivalents. Following that, various bivariate scatter plots of the statistical parameters were plotted and used to distinguish between the depositional settings. Furthermore, the modified linear discriminant function (LDF) of Sahu [32], modified C-M pattern of Passega [33] and log-probability curves of Visher [18] were used to deduce the modes of transportation and depositional processes.

Table 1. Co-ordinates and total drilling depth of the studied exploration wells

Wells/borehole	E-AH1	E-AJ1	E-BA1	E-BB1	E-D3
Co-ordinates	Latitude 35°11'13.40" S Longitude 21°08'37.07"E	Latitude 35°20'09.15" S Longitude 21°58'37.45"E	Latitude 35°09'29.67" S Longitude 21°28'31.19"E	Latitude 35°14'51.32" S Longitude 21°41'41.088"E	Latitude 35°28'45.91" S Longitude 21°56'16.16"E
KB to sea level (m)	26	26	22	22	186
Water depth (m)	91	142	115	122	156
Total drilling depth (m)	3729	3490	3130	3320	3996
No of samples	8	27	11	38	8

Table 2. Textural parameters and their corresponding verbal terms [10]

Standard deviations ( $\sigma$ )		Skewness ( $sk_1$ )		Kurtosis ( $kg$ )	
Phi standard deviation	Verbal sorting	Calculated skewness	Verbal skewness	Calculated kurtosis	Verbal kurtosis
< 0.35 $\phi$	very well sorted	> 0.30	strongly fine skewed	< 0.67	very platykurtic
0.35 – 0.50 $\phi$	well sorted	0.30 – 0.10	fine skewed	0.67 – 0.90	Platykurtic
0.50 – 0.71 $\phi$	moderately well sorted	0.10 – -0.10	near symmetrical	0.90 – 1.11	Mesokurtic
0.71 – 1.00 $\phi$	moderately sorted	-0.10 – -0.30	coarse skewed	1.11 – 1.50	Leptokurtic
1.00 – 2.00 $\phi$	poorly sorted	< -0.30	strongly coarse skewed	1.50 – 3.00	very leptokurtic
2.00 – 4.00 $\phi$	very poorly sorted			> 3.00	extremely leptokurtic
> 4.00 $\phi$	extremely poorly sorted				

## 4. Results and interpretation

### 4.1. Stratigraphy

The hydrocarbon target for borehole E-AH1 is the stratigraphically trapped sandstones within the 13A horizon (F-to-E interval). The targeted sandstone was encountered at 2452 m, and two cores (Cores 1 and 2) were cut between the depths of approximately 2471 m and 3161 m. Core 1 was cut from a depth of 2471 m down to 2485 m (14 m thick) and it consists of fine to medium-grained sandstones with shale interbeds, while core 2 was cut from a depth of 3149 m to 3160. It is 90 m long and 11.90 m thick, made up of ripple-laminated sandstone and mudstone. However, the core 2 is unavailable (missing) for this study. The main distinctive features in core 1 are that the sandstone is glauconitic and that there are shell fragments and sediment injection features (shale into sandstone) in the sandstone. Furthermore, the medium-grained sandstone and claystone contacts are erosional.

The E-AJ1 borehole was drilled to test for hydrocarbons within the stratigraphically trapped sandstones in the 10A to 14A horizons or interval (CEI-to-E interval). In borehole E-AJ1, six cores (Cores 1 to 6) were cut in borehole E-AJ1; however, only cores 1, 2, 3 and 4 are available for core logging. Core 1 (2701 – 2705 m) and core 2 (2720 – 2730.5 m) were cut in the targeted sandstone within the 14At1 horizon. Core 3 (2967 – 2984.9 m) was cut in the sandstone within the 12At1 and 11At1 horizons, while core 4 (3037 – 3043 m) intersected tight interbedded sandstones within the 10At1 horizon. Generally, cores 1 and 2 are predominantly fine to medium-grained sandstones, whereas cores 3 and 4 are made up of sandstones with shale interbeds. The sandstones are typically structureless, but in very few instances, the sandstones are having faintly horizontal to sub-horizontal stratification and dewatering structures. The hydrocarbon target for borehole E-BA1 is the stratigraphically trapped sandstones within the 9A and 13A horizons. The primary targeted sandstones were intersected at 2792

m, and two cores were cut from 2828 m to 2850 m. Core 1 (2828 – 2834 m) intersected the sandstone within the 13A horizon, whereas core 2 (2834 – 2850 m) was cut in sandstones within the 9A and 13A horizons. In general, core 1 is about 6 m thick and consists of shale with interlamination of sandstones and siltstone, whereas core 2 is made up of sandstone, conglomerate and mudstone, with a maximum thickness of about 16 m.

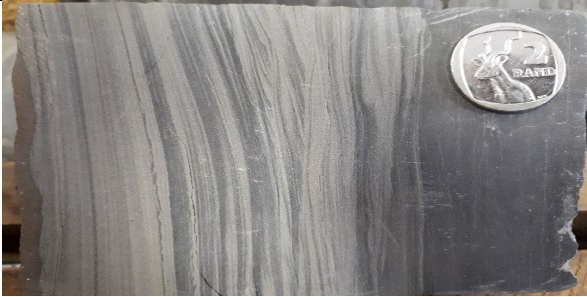
The borehole E-BB1 was drilled to evaluate the reservoir properties at various target horizons. The primary targets for hydrocarbons are the stratigraphically trapped sandstones in the 14A, 13A, 9A and Pre-6A horizons. Eight cores (Cores 1 to 8) were cut in borehole E-BB1, cores 1 to 6 and core 8 were investigated, while core 7 was not available (missing) for the core logging. The core 1 (2537.0 – 2537.6 m) and core 2 (2537.5 – 2556.0 m) were cut in sandstone within the 14A horizon. Core 3 (2659.0 – 2669.0 m) and core 4 (2719.5 – 2724.5 m) intersected the sandstone within the 13A horizon, while core 5 (2846.0 – 2864.0 m) and core 6 (2872.0 – 2877.0 m) intersected the sandstone within the 9A horizon. Core 8 (3280 – 3297.0 m) was cut in the sandstones below the 6A horizon. The sandstones in cores 1 to 4 are very lithic (with claystone and quartzite clasts), glauconitic, micaceous, slightly shelly, and carbonaceous. The sandstones in cores 5 and 6 are massive and carbonaceous, and contain quartzite and claystone clasts, whereas the sandstones in core 8 are very lithic, with abundant claystone and quartzite clasts. The hydrocarbon target for borehole E-D3 is the stratigraphically trapped sandstones within the 13A horizon (F-to-C interval). The targeted sandstones were intersected at 3252 m, and three cores (Cores 1, 2 and 3) were cut between the depths of approximately 3260 m and 3742 m. Core 1 (3260 – 3270 m), core 2 (3526 – 3530 m) and core 3 (3733 – 3742 m) are mostly made of fine to medium-grained massive sandstones with minor shale and siltstone interbeds. The stratigraphic description of the studied cores in boreholes E-AH1, E-BA1, E-AJ1, E-BB1, and E-D3 is shown in the supplementary data (Figure A1-A5).

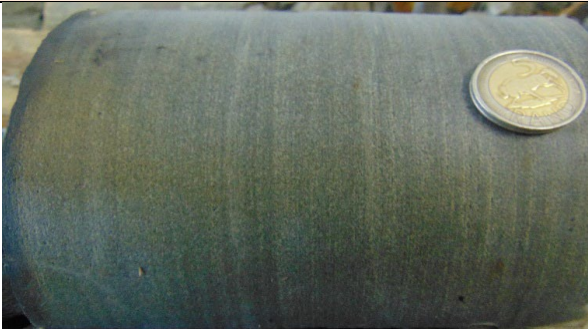
#### 4.2. Lithofacies

Thirteen different types of lithofacies were observed in the cores and they are presented in Table 3.

Table 3. Lithofacies identified in the southern Bredasdorp Basin

Facies code	Facies	Photograph	Descriptions
Gmm	Massive, matrix supported conglomerate		Colour: Light brownish grey to reddish grey. Matrix: Clay to silt Clasts: granule to pebble size Sorting: Poorly sorted Roundness: Subangular to sub-rounded Structure: Massive bedding
Sm	Massive (fine to medium) sandstone		Colour: Light to dark grey Grain size: Very fine to medium grained Structure: Faint lamination or massive bedding and sometimes bioturbated

Facies code	Facies	Photograph	Descriptions
Sr	Ripple cross-laminated sandstone		<p>Colour: Light grey            Grain size: Fine to medium grained            Structure: Ripple marks, cross lamination</p>
Sh	Horizontally stratified sandstone		<p>Colour: Light grey            Grain size: Fine to medium grained            Structure: Horizontal stratification, low angle cross-bedding and lenticular bedding (right)</p>
Smp	Massive to poorly stratified sandstone		<p>Colour: Light grey to dark grey            Grain size: Fine to medium grained            Structure: Massive bedding and faint stratification</p>
Sb	Bioturbated sandstone		<p>Colour: Dark grey            Grain size: Very fine to fine grained            Structure: Bioturbation</p>
Sl	Parallel-laminated sandstone		<p>Colour: Light grey to dark grey            Grain size: very fine to medium grained            Structure: Parallel lamination or wave lamination (left)</p>

Facies code	Facies	Photograph	Descriptions
Sml	Massive to faintly laminated muddy sandstone		<p>Colour: Light to dark grey            Grain size: Clay-size to fine grained sand            Structure: Massive bedding or faint lamination</p>
Fsm	Massive siltstone and mudstone		<p>Colour: Light to dark grey            Structure: Massive bedded and sometimes with small ripples</p>
Fms	Thin-bedded muddy (clay-rich) siltstone		<p>Colour: Light grey            Structure: Thin-bedded, with erosional surface</p>
Fmb	Massive mudstone, occasionally laminated or bioturbated (right middle)		<p>Colour: Dark grey            Structure: Massive bedding, bioturbation, occasionally laminated</p>
Fc	Laminated carbonaceous shale and mudstone		<p>Colour: Dark grey to black            Structure: Lamination, thin bedding and rich in carbonized plant matter</p>

Facies code	Facies	Photograph	Descriptions
FI	Laminated silt-stone/shale		Colour: Light to dark grey Structure: Lamination, ripple lamination with few lenticular bedding (bottom left)

### 4.3. Grain size statistics

The four statistical parameters used to depict the textural characteristics of the Bredasdorp Basin sediments are the mean ( $M_z$ ), standard deviations ( $\sigma_I$ ), skewness ( $Sk_I$ ) and kurtosis ( $K_G$ ). The calculated mean values for the Bredasdorp Basin sandstones in boreholes E-AH1, EAJ1, E-BA1, E-BB1 and E-D3 range between 1.33 $\phi$  to 2.33 $\phi$ , 1.32 $\phi$  to 3.31 $\phi$ , 1.28 $\phi$  to 3.31 $\phi$ , 1.19 $\phi$  to 3.29 $\phi$  and 2.31 $\phi$  to 3.29 $\phi$ , respectively (Figures 3-7). Furthermore, the average mean grain size values in boreholes E-AH1, E-AJ1, E-BA1, E-BB1 and E-D3 are 1.95 $\phi$ , 2.18 $\phi$ , 2.17 $\phi$ , 2.19 $\phi$  and 3.20 $\phi$ , respectively. These average values indicate that fine sands predominate, but each borehole exhibits local variations ranging from medium-grained to fine-grained sands. Generally, the observed changes in the mean grain size are due to instabilities in the energy conditions during the sediment deposition. The fine grain nature may reveal the basin's moderately low energy condition at the time of deposition. On the other hand, the intermittent occurrence of the medium-grained sand (massive sandstone) could be due to limited inputs and a sudden increase in energy conditions [34].

The standard deviation values of the studied samples ranges from 0.50 $\phi$  to 0.86 $\phi$  in the variable scale of Folk [10], indicating moderately well sorted to moderately sorted (Figures 3-7). Most of the studied samples are moderately well sorted and the predominance of moderately well sorted sediments could be due to repeated back and forth movement or winnowing action by the depositing agent as well as additional incursion of hitherto sorted sediments in the depositional environment [9,35]. The calculated graphic skewness values for the samples vary from -0.22 to 0.16, indicating coarse-skewed to fine-skewed (Figures 3-7). The calculated skewness values range from negative to positive, indicating the presence of finer and coarser fractions. In general, the presence of near symmetrical and fine-skewed sediments indicates the start of fine material deposition and the removal of coarser portions. These near-symmetrical sediments imply moderate energy conditions in the depositional environment, whereas the finely skewed sediments imply extensive winnowing or longer sediment transport [36]. The lack of extreme conditions such as wave breaking, tidal variations, and seasonal supply of detrital materials could explain the dominance of near symmetrical sediments.

The graphic kurtosis values for the samples studied range from 0.87 to 1.21, indicating that they are platykurtic to leptokurtic and mostly mesokurtic (Figures 3-7). The mesokurtic to leptokurtic nature of the studied samples suggests that finer fractions or materials are constantly added after the depositing agent's winnowing action and that their original or initial characteristics are preserved during deposition. The dominance of mesokurtic character indicates that the better-sorted sediments were laid down by a one-way current flow, allowing the sediments to settle in a lower energy environment. Similarly, the leptokurtic character of the studied samples indicates fluctuations in energy conditions during deposition. Variations in kurtosis values may be caused by changes in the flow characteristics of the transport and depositional medium. The presence of fine sand-size particles with mesokurtic to platykurtic characteristics, as well as the roundness of the grains, indicates sand maturity, which could be due to the accumulation of fine sand-size materials in a low-energy environment.

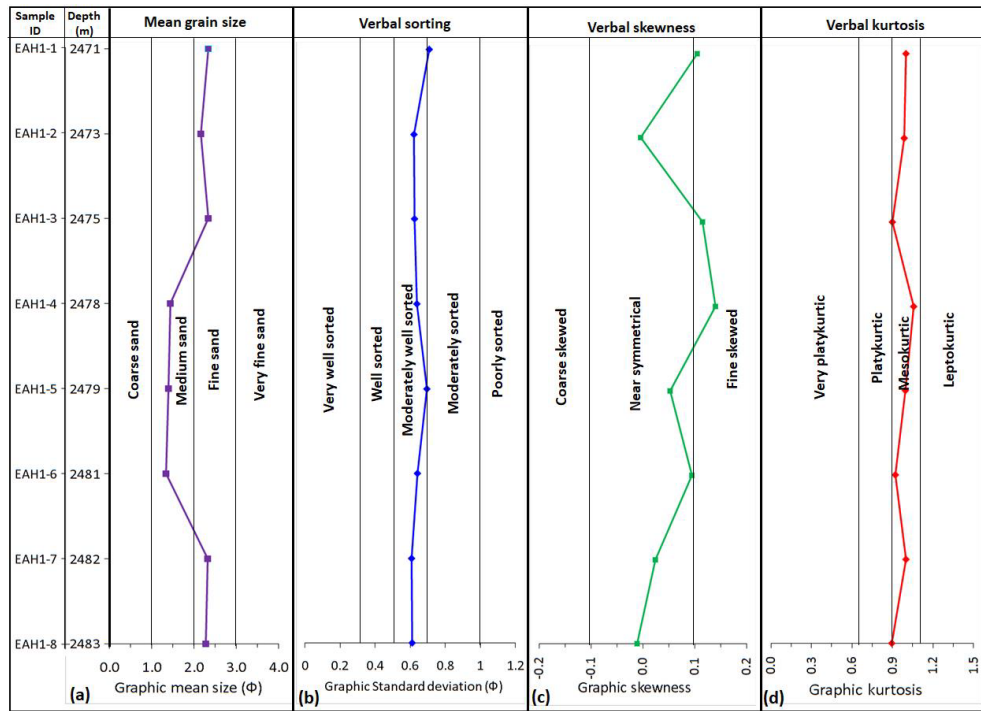


Figure 3. Downhole plot of the textural parameters of the Cretaceous sandstones from the Borehole E-AH1: (a) Graphic mean or grain sizes; (b) standard deviation or sorting; (c) skewness; (d) kurtosis

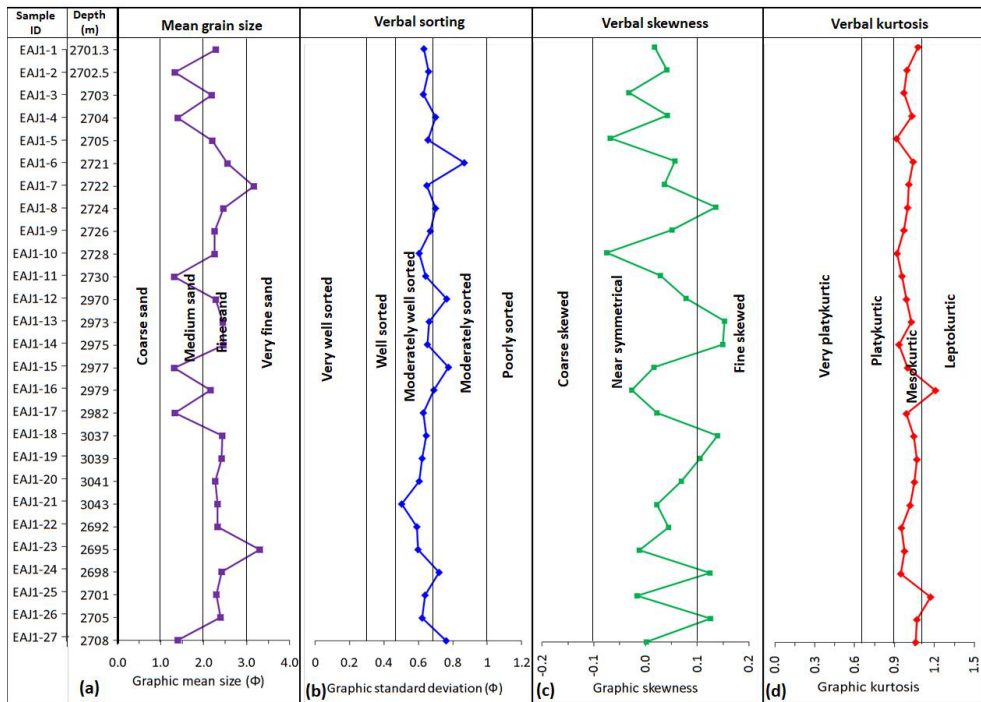


Figure 4. Downhole plot of the textural parameters of the Cretaceous sandstones from the Borehole E-AJ1: (a) Graphic mean or grain sizes; (b) standard deviation or sorting; (c) skewness; (d) kurtosis.

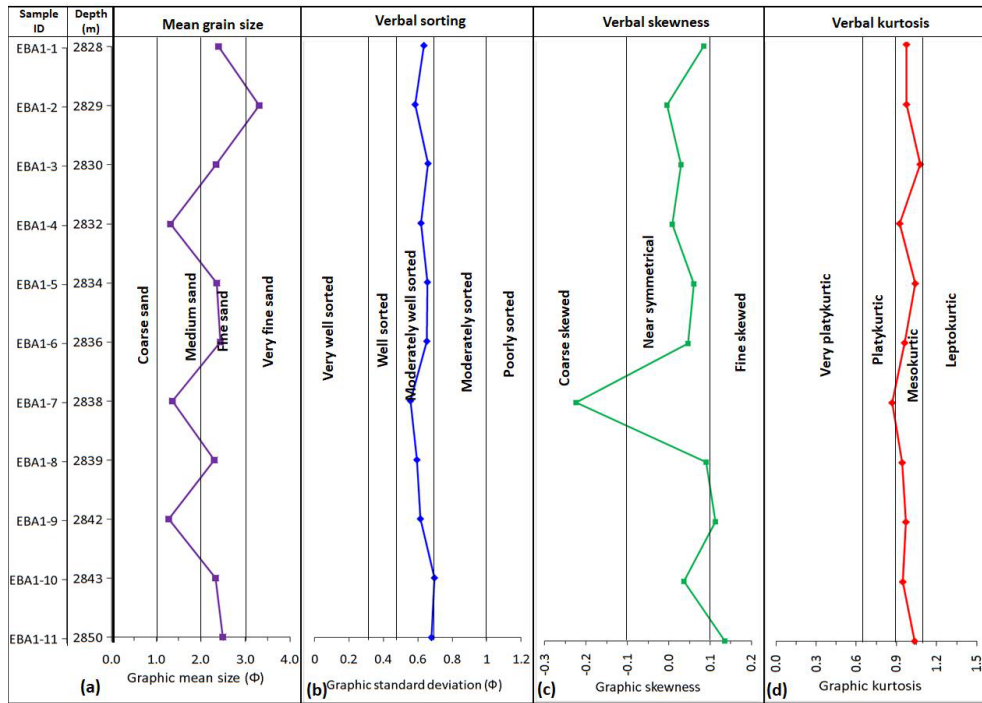


Figure 5. Downhole plot of the textural parameters of the Cretaceous sandstones from the Borehole E-BA1: (a) Graphic mean or grain sizes; (b) standard deviation or sorting; (c) skewness; (d) kurtosis

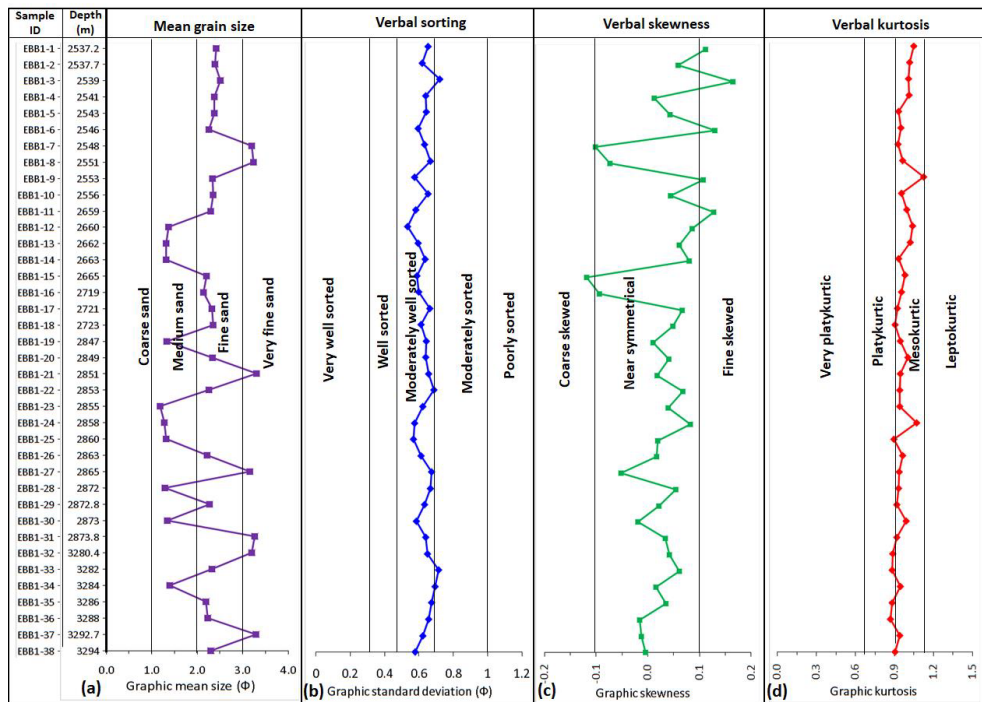


Figure 6. Downhole plot of the textural parameters of the Cretaceous sandstone samples of the Borehole E-BB1: (a) Graphic mean or grain sizes; (b) standard deviation or sorting; (c) skewness; and (d) kurtosis

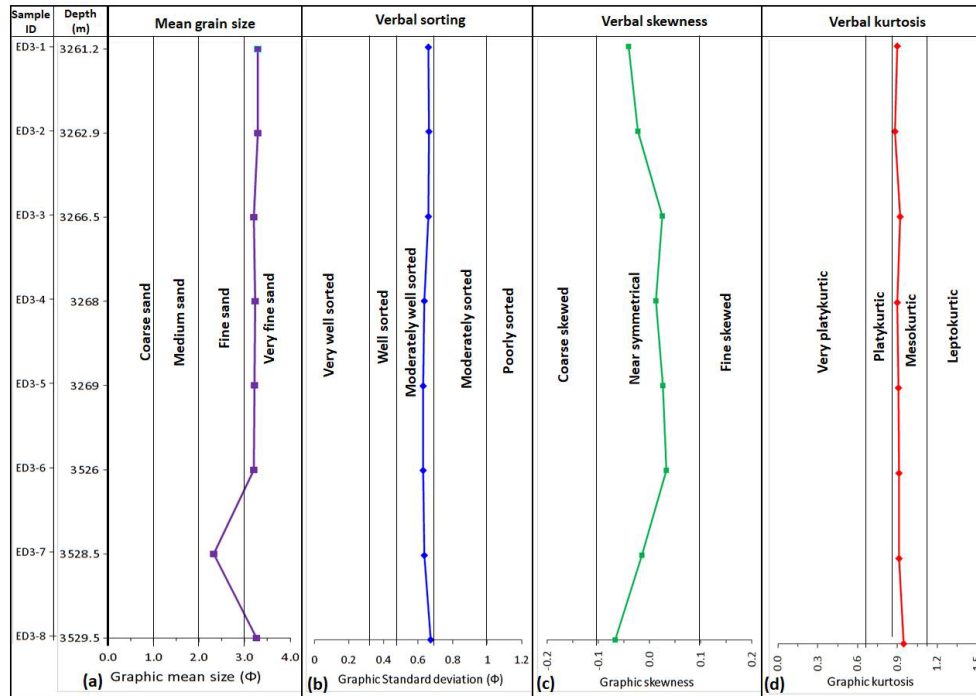


Figure 7 Downhole plot of the textural parameters of the Cretaceous sandstones from the Borehole E-D3: (a) Graphic mean grain sizes; (b) standard deviation or sorting; (c) skewness; (d) kurtosis

#### 4.4. Depositional processes and environments

##### 4.4.1. Bivariate scatter plots

The bivariate scatter plots of the statistical parameters (i.e., mean, skewness, and kurtosis) were used to decipher the depositional processes and settings [13, 29, 37-38]. The bivariate plot of mean versus skewness is best used to distinguish between river processes, dune processes, and wave processes.

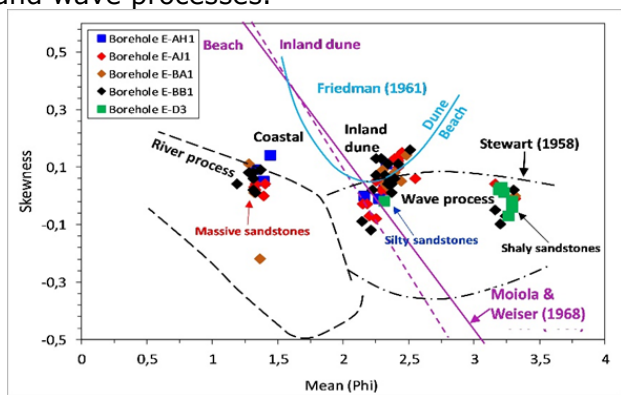


Figure 8. Cross plot of skewness against mean showing coastal dune, wave and river processes (Background fields after [13,29,37])

Moiola and Weiser [13] acknowledged that Friedman's [29] discriminating boundary does distinguish between modern inland dunes and river sands. The bivariate plot of mean versus skewness (Figure 8) shows that the wave process environment contains most of the samples, followed by the river process environment. Furthermore, most of the samples were plotted in the coastal environments described by [29] and [13]. This bivariate diagram shows plots that overlap, possibly indicating the multiple influences of river, dune, and beach environmental conditions.

##### 4.4.2. C-M pattern (Passega diagram)

Passega [39] proposed the C-M plots as a mechanism for interpreting the hydrodynamic conditions or forces at work during sediment deposition. The plot depicts the relationship between "C," the coarsest one percentile value of the grain size distribution in microns, and "M," the log-probability scale's median value in microns. Because the coarse fraction of sediment is more representative of the depositional agent than the fine fraction, these parameters were

chosen [33]. The Passega diagram includes several fields that correspond to different transport and sedimentation conditions in the marine, littoral, or fluvial domains, such as pelagic suspension (T field), uniform suspension (SR field), gradual suspension (QR field), suspension and rolling (QP field), rolling and suspension (PO field), and rolling (ON field). Figure 9a shows samples from borehole E-AH1 plotted in both rolling (NO) and rolling and suspension (OP). Borehole E-AJ1 samples are found in the rolling (NO), rolling and suspension (OP), and suspension and rolling (PQ) sections, whereas samples from borehole E-BA1 are found in the suspension and rolling (PQ) section. The samples from borehole E-BB1 are plotted in both rolling (NO) and suspension and rolling (PQ), whereas the majority of the samples from borehole E-D3 are in uniform suspension (RS). The majority of the samples studied are projected in the PQ (suspension and rolling), PO (rolling and suspension), NO (rolling), and QR fields (gradual suspension). The main section of a river channel is defined by the PQ field. The samples projected in the PO field represent the lower size limit of grains transported by rolling, while the samples projected in the QR field represent samples deposited by shallow braided streams and sandbars adjacent to the main currents of larger stream channels. The increase in the C parameter indicates that the energy levels of the depositional environment currents have increased. As a result of the plot, a significant number of samples are representative of deposition in low energy environments. Overall, turbidity controls influenced the rolling and suspension of sediments, indicating that the river transportation process was intensive, particularly in the main channels. Furthermore, the C-M plot (Figure 9b) shows seasonal variations in energy conditions. The plot shows that all the samples are projected between environments 4 and 5, which represent tractive current and beach. Tractive currents typically transport sediments by rolling and sliding along both the riverbed and the beach.

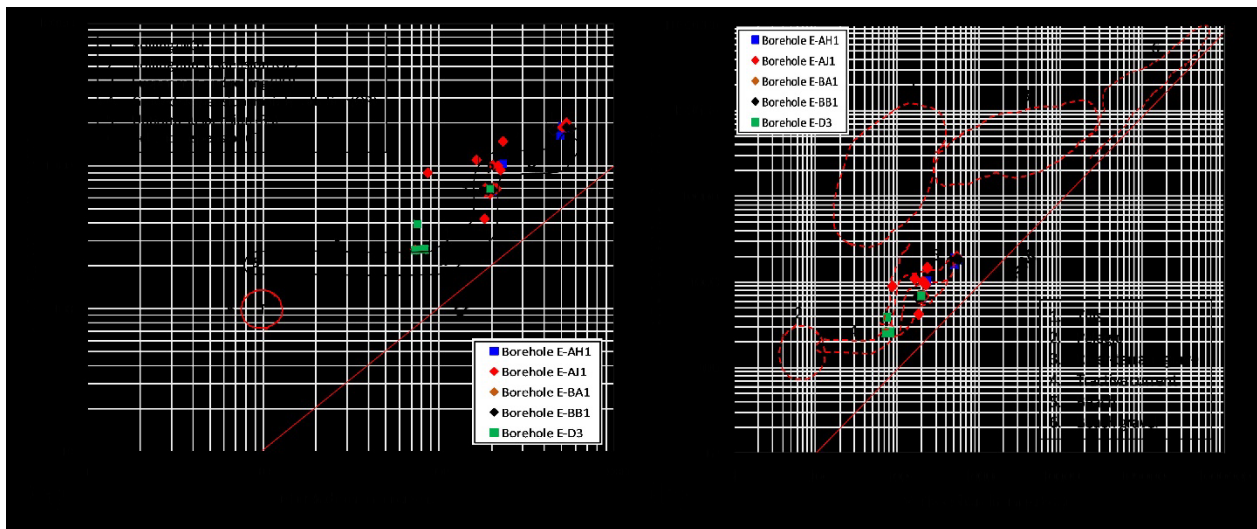


Figure 9. (a) C-M diagram showing the mode of transportation for the Bredasdorp Basin sandstones (background field after [33]); (b) C-M diagram showing that the Bredasdorp Basin sandstones are tractive current and beach deposits (background field after [33])

#### 4.4.3. Visher diagram

Visher's [18] log-probability curves were used to differentiate between traction, saltation, and suspension load in the Bredasdorp Basin sediments. The Visher plot for the sandstones in boreholes E-AH1, E-AJ1, E-BA1, E-BB1, and E-D3 (Figure 10) revealed a predominance of double saltation (saltation I and II) populations with only one suspension population. The saltation and suspension populations can reach up to 80% and 20%, respectively. The saltation I and II populations were frequently truncated between  $1.5\phi$  and  $2.5\phi$ , which could be attributed to internal forces that initiated rolling or sliding along the sea floor [18]. In comparison to the suspension population, the saltation I and II populations are moderately well-sorted. In fact, the suspension load was not sorted during deposition; it was deposited by

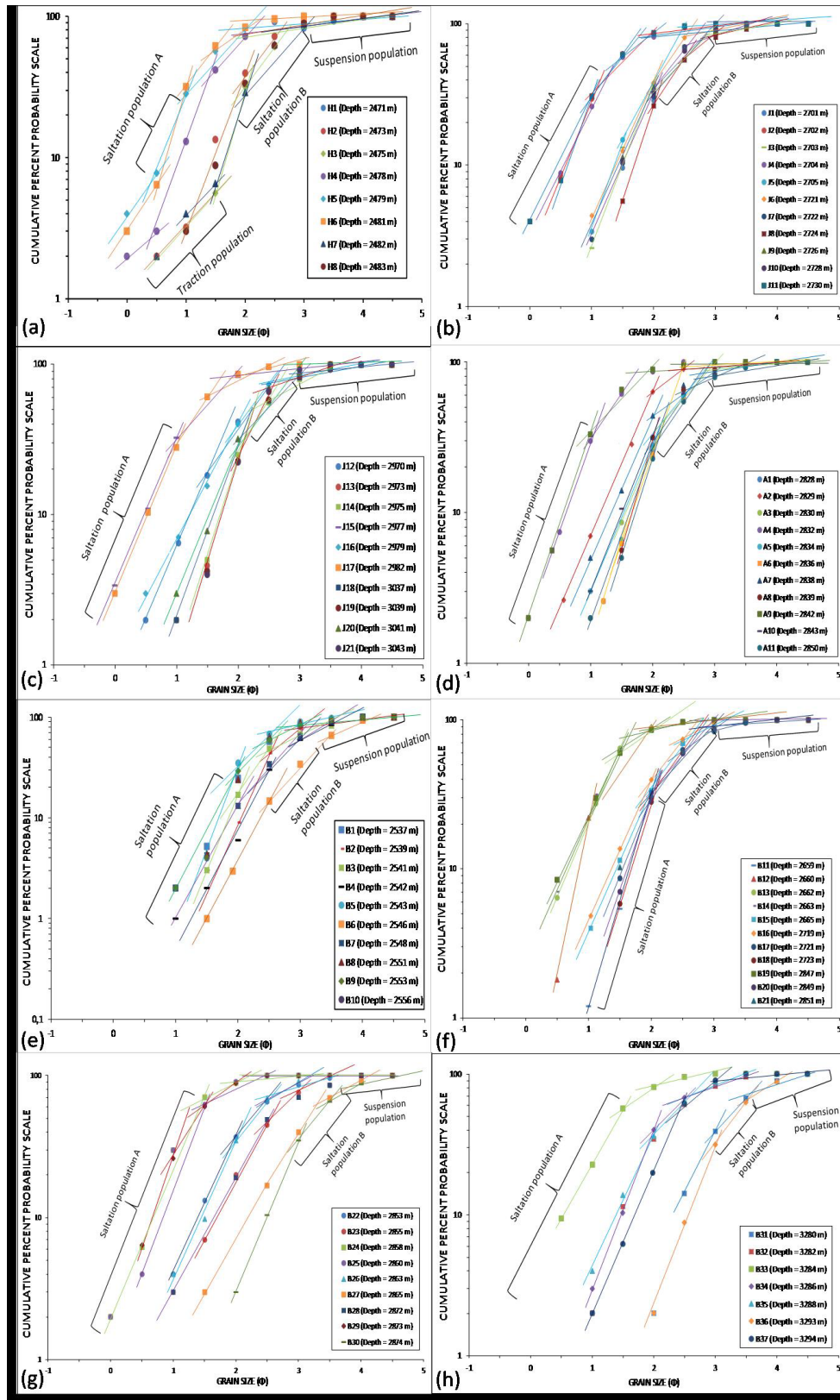


Figure 10. Log-probability weight percentage frequency curves showing the double saltation and single suspension and traction populations for (a) Borehole E-AH1; (b-c) Borehole E-AJ1; (d) Borehole E-BA1; (e-g) Borehole E-BB1; (h) Borehole E-D3

gravity sinking from the suspension mud. The log probability curves (Figure 10) are like those of ancient and modern marine sediments proposed by [18], where both saltation (saltation I and II) and suspension populations predominate. Two saltation populations are typically associated with the tidal environment, where both flow and ebb currents are active at the same time.

**4.4.4. Linear discriminate function (LDF)**

The application of linear discriminate functions as a tool for interpreting changes in energy and fluidity factors during sediment deposition appears to have a strong relationship with the various depositional processes and environments [32]. Sahu [32] distinguished between shallow agitated water and beach, beach and shallow marine, shallow marine and deltaic or lacustrine, and turbidity and deltaic using LDFs of Y1, Y2, Y3, and Y4. Equations i-iv show the mathematical expressions for Y1, Y2, Y3, and Y4. M, r, SK, and KG in the equations represent mean grain size, standard deviation, skewness, and kurtosis, respectively.

$$Y_1 = -3.5688M + 3.7016r^2 - 2.0766SK + 3.1135KG \quad (i)$$

If Y1 is greater than -2.7411, the environment is beach, and if Y1 is less than -2.7411, the environment is shallow agitated water.

$$Y_2 = 15.6534M + 65.7091r^2 + 18.1071SK + 18.5043KG \quad (ii)$$

The environment is shallow marine if Y2 is greater than -63.3650, and if Y2 is less than -63.3650, the environment is beach.

$$Y_3 = 0.2852M - 8.7604r^2 - 4.8932SK + 0.0482KG \quad (iii)$$

If Y3 is greater than -7.4190, the environment is shallow marine and if Y3 is less than -7.4190, the environment is lacustrine or deltaic.

$$Y_4 = 0.7215M - 0.4030r^2 + 6.7322SK + 5.2927KG \quad (iv)$$

If Y4 is greater than 9.8433, it suggest deltaic deposition, and if Y4 is less than 9.8433, it signify turbidity current deposition.

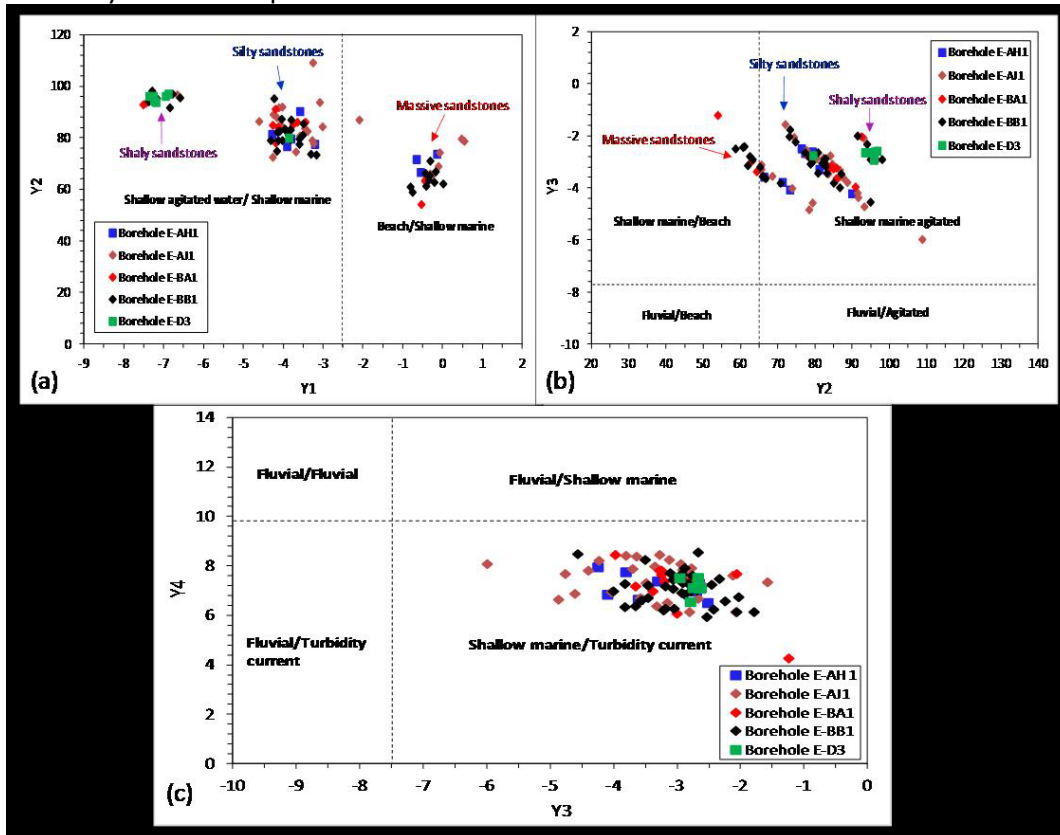


Figure 11. Linear discrimination functions (LDF) binary plot of (a) Y1 against Y2; (b) Y2 against Y3; (c) Y3 against Y4, showing depositional environments and process for the Bredasdorp sandstones [32]

For the Bredasdorp sandstones, the calculated Y1, Y2, Y3, and Y4 values range from -7.50 to 0.48, 54.01 to 108.85, -6.00 to -1.24, and 5.92 to 8.54, respectively. The Y1 values of samples from boreholes E-AH1, E-AJ1, E-BA1, and E-BB1 indicate that the massive sandstones are beach process, whereas the shaly and silty sandstones are agitated water process. In terms of Y2 values, all shaly and silty sandstones are found in shallow marine environments, while approximately 65% of massive sandstones are found in shallow marine environments and the remaining 35% on the beach. In terms of Y3 and Y4 values, all the samples examined were plotted in the shallow marine environment and turbidity current deposits, respectively. Furthermore, the bivariate plot of Y2 against Y1 (Figure 11a) shows that the majority of the samples (about 80%) fall in the shallow agitated water area, about 12% fall in the beach/shallow agitated water area, and the remaining samples (about 8%) fall in the beach/beach environment. Figure 11b shows that approximately 90% of the samples are from shallow agitated marine environments, while the remaining 10% are from shallow marine/beach environments. The binary plot of Y4 versus Y3 revealed that the Bredasdorp sandstones are shallow water marine/turbidity current deposits (Figure 11c).

#### **4.4.5. Lithofacies associations (FAs)**

##### **4.4.5.1. Matrix supported conglomerate and massive sandstone, FA1 (Gmm + Sm)**

FA 1 is composed of Gmm and Sm facies. The Sm facies is found in all boreholes, but the Gmm facies is only found in borehole E-BA1. The Gmm facies is a matrix-supported polymictic conglomerate that ranges in colour from light brownish to reddish grey. This Gmm facies is approximately 4 m thick with a fine upward sequence. Furthermore, the lower and upper surfaces of the Gmm facies are erosional. The matrix of the Gmm facies is claystone and fine- to medium-grained glauconitic and calcareous sandstone. The Gmm facies is poorly to moderately well sorted, with the pebble-sized clasts at the bottom and the smaller clasts at the top. The pebbles range in shape from sub-angular to well-rounded (sometimes elongated). The clasts in the Gmm facies are frequently not in contact, but on a few occasions, the clasts are feebly connected and range in diameter from 2 cm to 10 cm. Shell fragments are also found in the sandstones and pebbles. The Sm facies is made up of fine- to coarse-grained sands. The Sm facies has fine to coarse-grained sands that are mostly grey with brownish and dark grey colorations. The Sm facies is massive, but it does occasionally show faint low angle bedding. The thickness of a single or individual Sm bed ranges from about 4 cm to 6 m. The contact between the Sm facies and the overlying and underlying facies is frequently sharp, but gradational and erosional contacts can also be found. The Sm facies also contains soft-sediment deformation structures (i.e., dish structures).

FA1 contains many erosional surfaces with undulating or flat surfaces, which is a characteristic of channel deposits; thus, FA 1 represents channel deposits. The Gmm facies is characterized by high-energy conditions associated with channel fills. The Sm facies is thought to be channel-fill sandstone that accumulated on a submarine fan. The angular nature of the clast, as well as the presence of large pebbles in the Gmm facies, may indicate that the Gmm facies is close to the source area and that it was deposited under high-energy conditions. Shell fragments and glauconite in the Sm facies indicate deposition in a marine environment. FA 1 is thought to be submarine channel deposits. This interpretation was made based on the erosive nature of the claystone/conglomerate contact and the massive nature of the sandstone.

##### **4.4.5.2. Ripple cross-laminated, trough cross-bedded and bioturbated sandstone, FA 2 (Sr + Sh + Sb)**

The FA 2 is composed of the Sr, St, Sh, and Sb facies, which are mostly sub-angular to rounded, moderately to well sorted, and fine- to medium-grained sandstones. The Sr facies is found in boreholes E-BB1 and ED3 and is found in moderately well-sorted fine-grained sandstones ranging in colour from light grey to dark grey. Ripple cross-laminations are frequently observed above parallel to sub-parallel laminations in borehole E-BB1. The Tb interval is associated with parallel and sub-horizontal lamination, whereas the Tc interval is associated with

ripple cross-lamination. The St facies is most common in borehole E-BB1 but occasionally present in boreholes E-BA1 and ED3. It is composed of light brownish grey medium-grained and well sorted sandstone with tangentially inclined cross bedding with "u" shaped basal dune surfaces visible at certain angles and with erosive and scoured bases. Some of the trough cross-bedded units in the FA2 are bioturbated (Sb facies). This Sb facies is distinguished by a light-to-dark grey, structureless to thinly bedded, highly disrupted sandstone containing numerous shell fragments. The Sh facies is a light grey, fine-to-medium-grained, moderately well-sorted sandstone that is present in all five boreholes. The lower and upper contacts of rock units and beds are mostly non-erosional, and the strata show a tabular geometry.

The Sr and St Facies are formed due to the unidirectional flow of the transporting medium. According to Miall [41], the St Facies is formed by sand movement from sinuous to mega-ripples and dune by comparatively fast flowing currents. The ripple cross-laminations in the Sr facies are usually traction features caused by unidirectional currents transporting bedload during deposition (i.e., river or turbidity currents). These traction features may indicate that FA 2 was deposited by river flows that separated from medium-to-high-density turbidity currents [40]. Pemberton *et al.* [41] demonstrated that the Sb facies are soft ground and substrate-controlled, and that they form as a result of biogenic reworking in low to medium energy marine environments. The Sb facies is the result of constant reworking of overbank sands between channels [42]. FA 2 represents the deposits of a submarine channel-levee.

#### **4.4.5.3. Massive sandstone with mudstone and shale interbeds, FA 3 (Sm + Fmb + Fl)**

The FA 3 is present in all the boreholes, and it comprises the Sm, Fmb and Fl facies. The Sm facies is characterised by very fine-to medium-grained, well-sorted massive sands with sharp contacts (lower and upper contacts). The Sm beds are typically light grey in colour, but a dark grey colour can be found in some cores, particularly in borehole E-BA1. The Sm facies has a thickness ranging from 4 cm to 2 m, with individual sand interbeds ranging from about 20 mm to 60 cm. The Sm facies is generally structureless, but it does show faint stratification on rare occasions. Calcareous concretions and siltstone clasts are sometimes present within the structureless sandstones. In general, the thin sandstone beds show fining upwards into mudstone. The sand interbeds are horizontal but have uneven bounding or erosive surfaces. The Fmb facies is massive, bioturbated, and sometimes mottled, whereas the shale facies (Fl facies) is distinguished by its lamination. The Fl is mostly homogeneous, but in a few places, it has very thin siltstone laminae with an average thickness of about 4 mm. The Fmb and Fl facies are both dark grey in colour, with thicknesses ranging from 2 cm to approximately 1 m.

The alternation or interbeds of the Fmb, Fl, and Sm facies indicate that deposition took place under fluctuating energy conditions. The flat beds and laminations in the Fmb and Fl facies indicate calm waters and slow sediment settling. The sandstone beds, on the other hand, suggest rapid deposition under high hydrodynamic (water energy) conditions. The Fmb facies' high degree of bioturbation may be indicative of well-oxygenated marine bottom waters. Erosional remnants are thought to be the Sm facies with sharp or erosive bounding surfaces. FA 3 represents deposits that resemble submarine sheets. Related facies were interpreted by Saito and Ito [43] as sheet-like turbidite units. These facies are from unconfined turbidity currents in a submarine fan's middle and outer domains. Because the Sr and St are so close to FA 1 (channel-fills deposits), FA 1 is an off-axis or overbank deposit. The presence of FA 3 intercalating with alternated laminated sandstone and claystone lends support to this interpretation. Nonetheless, the possibility that FA 3 is a sheet-like deposit, as reported by Habgood *et al.* [44], remains. FA 3 is thought to be submarine sheet lobe deposits.

#### **4.4.5.4. Alternating laminated to interbedded sandstone/siltstone and mudstone FA 4 (Sl + Smp + Fl + Fsm)**

The FA 4 consists of the Sl, Smp, Fl, and Fsm facies. The Sl, Fl, and Fsm facies can be found in all boreholes, but the Smp facies can only be found in borehole E-BB1. Sl and Smp facies are typically medium grained and light grey in colour. The contact between Sl and Smp is gradational, whereas the contact between Fl and Fsm is sharp, but gradational in some cases.

The base of the Smp facies is planar but sometimes erosional. Both the Sl and Smp facies are mostly glauconitic and occasionally contain calcareous nodules and bioturbation. The thickness of the Sl and Smp facies varies between 2 cm and 1.3 m, with individual sand interbeds varying from about 5 mm up to 42 cm. Just like in the FA3, the sand interbeds in FA4 are horizontal and sometimes show uneven bounding surfaces. The Fmb and Fl facies are both dark grey in colour, with thickness varying from 12 cm up to 3.2 m. Calcareous concretions and bioturbation are observed in the Fl and Fsm facies.

The alternation of the Sl, Smp, Fl and Fsm facies also suggests that the deposition happened under fluctuating energy conditions. The laminations in the Fl facies indicate quiet waters and slow settling of the sediments, whereas the Sl and Smp facies are suggestive of fast deposition under high hydrodynamic (water energy) conditions. The Sl and Smp facies are interpreted to be the basal part of channel-fill sandstones deposited on a submarine fan in an inner fan to middle fan setting. The channelized inner fan to mid-fan environment is linked with the alternated Sl, Smp, Fl, and Fsm facies. Nonetheless, it is perhaps deposited in an overbank setting in a fan valley. The Fl and Fsm facies are derived from the settling of hemi-pelagic materials. These materials can blanket all areas of a fan, including the interchannel areas. The FA 4 is interpreted as submarine lobe fringe or overflow deposits.

#### **4.4.5.5. Massive mudstone with interlamination of clay-rich sandstone and siltstone, FA 5 (Fsm + Fmb + Fms + Sb + Sml)**

The FA 5 is made up of the Fsm, Fmb, Fms, Sb and Sml facies. The Fsm, Fms, Sb and Sml facies are present in all the boreholes, while the Fmb facies is only observed in borehole E AH1. In most cases, from the base to the top, the sandstone beds grade from fine-grained sandstone to laminated siltstone and mudstone. The contacts between the mudstone and siltstone are gradational, whereas the contacts between the mudrocks (Fsm, Fmb and Fms facies) and sandstones (Sml and Sb facies) are sharp. The Fsm and Fmb facies are characterised by massive, light to dark grey claystone. The claystone is mostly homogenous and intermittently interlaminated with clay-rich sandstones (Sml facies) and siltstone (Fsm and Fms facies). The Fsm and Fms facies are both grey in colour, with a thickness varying between 2.2 cm and 1.5 m. The Sml facies are largely massive and muddier (clay-rich) at the base and occasionally with rip-up mud clasts. The thickness of the Sml facies ranges from about 6.4 cm up to 3.1 m. Bioturbation is frequently observed in the Sb facies, whereas mud clasts, ripple laminations, and plant fragments are occasionally seen in the Sb facies.

The mudrock facies (Fsm, Fmb and Fms) indicate that sedimentation occurred by suspension fall-out in a quiet and reduced (anoxic) environment. The existence of thin sandy layers could be due to low-density turbidity currents. The alternation of mudrock and sandstone beds suggests that the deposition occurred under fluctuating energy conditions. Again, the alternation of laminated units with clay-rich units points to the fact that different kinds of low-density turbidity currents alternated within the water column. The laminations in the Fsm and Fms facies indicate quiet waters and slow settling of the sediments, while the Sb and Sml facies perhaps indicate fast deposition under high hydrodynamic (water energy) conditions. The mudrock facies is thought to have been deposited when turbidite systems are no longer active, for instance, when a starvation period prevails during the supply of sediments. FA5 is interpreted as basin plain deposits.

#### **4.4.5.6. Carbonaceous shale and mudstone with occasional siltstone laminae, FA 6 (Fc + Fl + Fms)**

The FA 6 comprises of the Fc, Fl and Fms facies and they are observed in all the boreholes. These mudrocks (Fl, Fc and Fms facies) have colour varying between light grey and black, and the contacts between the Fl, Fc and Fms facies are gradational. The Fc facies is fissile, organic-rich and black in colour, with thickness ranging between 2 cm and 2 m. Slickensides, plant fragments and burrows are occasionally seen in the Fc facies. The Fl and Fms facies are laminated with lenticular siltstone laminae within the mudstone. The thickness of these siltstone

laminae varies between 1 mm and 8 mm, while the thickness of the F1 and Fms facies ranges from about 1 cm up to 3.4 m.

The well laminated, very fine-grained size and black colour as well as the presence of organic carbon-rich shale (Fc facies) in FA 6 suggest that the deposition was by suspension sedimentation in a low-energy hydrodynamic condition, anoxic or reducing environment in which the water body is deep (i.e., deep ocean waters). The FA6 is interpreted as a pelagic-hemipelagic settling in a deep sea floor or plain setting or environment (basin plain deposits).

#### 4.5. Depositional model

The southern Bredasdorp Basin's lithofacies and grain size analyses revealed shallow marine and deep marine depositional environments. The depositional environment, as revealed by the facies analysis, consists of submarine channel deposits (FA 1: matrix-supported conglomerate and massive sandstone). The FA 2 submarine channel-levee deposit is made up of (ripple cross-laminated, trough cross-bedded, stratified and bioturbated sandstone). FA 3 (massive sandstone with interbeds of mudstone and shale) represents a submarine sheet lobe, whereas FA 4 (alternating laminated to interbedded sandstone/siltstone and mudstone) represents submarine lobe fringe deposits. FA 5 (massive mudstone with minor interlamination of clay-rich sandstones and siltstone) and FA 6 (carbonaceous shale and mudstone with occasional siltstone laminae) are basin plain deposits. Figure 12 depicts the proposed depositional model for the southern Bredasdorp Basin. Megner-Allogo [45] reported that the marine sediments of the Bredasdorp Basin were deposited in a submarine to abyssal plain (deep sea) setting, which the conceptual model confirms or agrees with.

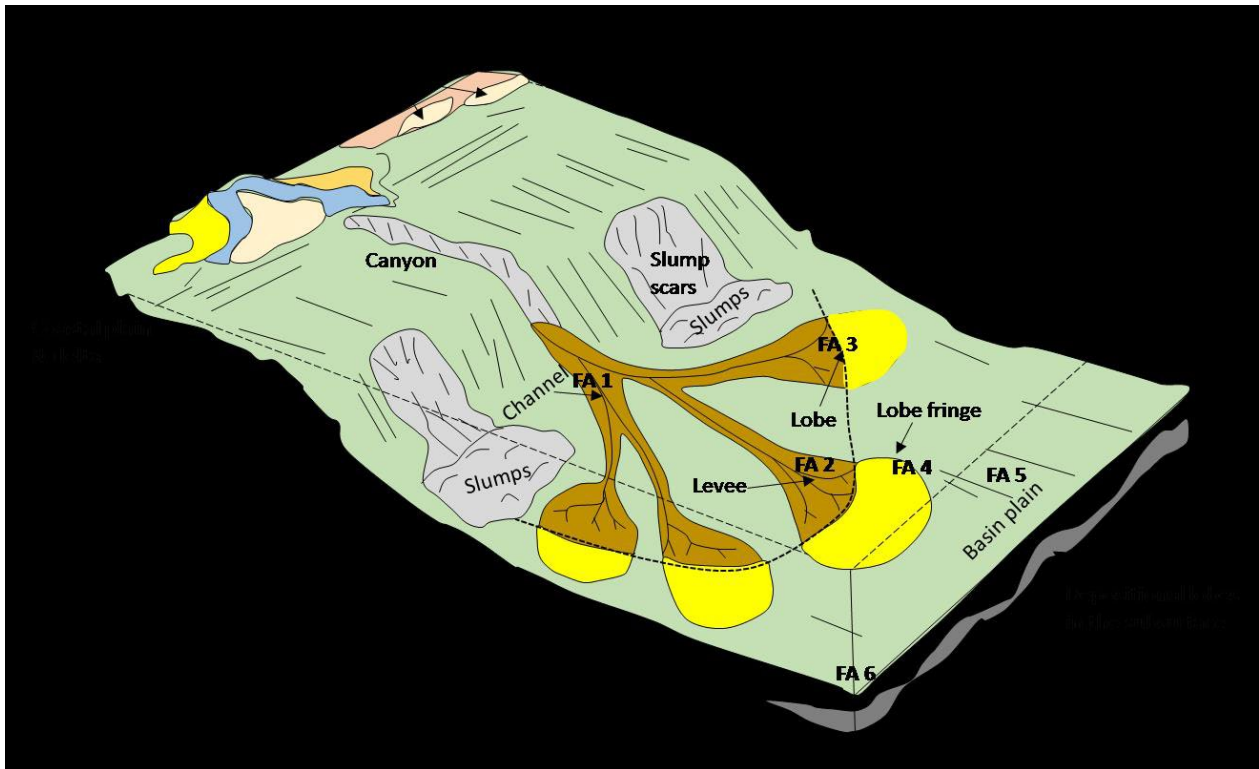


Figure 12. Proposed depositional model for the southern Bredasdorp Basin. The model shows that FA 1, FA 2, FA 3, and FA 4 are shallow marine deposits, while FA5 and FA 6 are deep marine deposits

#### 5. Discussion

Lithofacies analysis of the cores was performed to describe the rock units and to unravel their depositional environments. Thirteen lithofacies were identified and classified into six dis-

tinct facies associations (FAs). The identified FAs are as follows: FA 1: Matrix supported conglomerate and massive sandstone (Gmm + Sm), FA 2: Ripple cross-laminated, trough cross-bedded, and bioturbated sandstone (Sr + St + Sh + Sb), FA 3: Massive sandstone with mudstone and shale interbeds (Sm + Fmb + Fl), FA 4: Alternating laminated to interbedded sandstone and mudstone (Sl + Smp + Fl + Fsm), FA 5: Massive mudstone with minor interlamination of clay-rich (muddy) sandstones and siltstone (Fsm + Fmb + Fms + Sb + Sml) and FA 6: Carbonaceous shale and mudstone with occasional siltstone laminae (Fc + Fl + Fms). Sedimentological evidence from facies interpretation indicates that FA1, FA2, FA3, FA4, FA5 and FA6 are submarine channel-fills, submarine channel-levees, submarine sheet lobes, submarine lobe fringes/overflow, basin plain deposits, and deep sea floor/basin plain deposits, respectively. Furthermore, the carbonaceous shale and sandstone facies may be potential source and reservoir units important for petroleum generation and hosting.

The Bredasdorp Basin sandstones' grain size analysis was used to unravel and understand their mechanisms of transportation and hydrodynamic environments. According to the grain size distribution, the majority of the Bredasdorp Basin sandstones are fine-grained, moderately well-sorted, mesokurtic, and nearly symmetrical. The fine arenaceous texture of the sandstones indicates that the depositional environment is moderately low energy. The well-sorted to moderately well-sorted nature of the sediments suggests winnowing and back and forth movement of the depositing agents. The dominance of the near symmetrical category may indicate riverine input and mixing of similar modal fractions. The linear discriminant functions (LDF) analysis reveals that the sandstones are turbidity current deposits formed by coastal dune and beach processes in a shallow marine environment. The Passega Diagram (C-M pattern) reveals that these sandstones were mostly deposited by rolling, rolling and suspension, suspension and rolling, and uniform suspension processes. Furthermore, the Passega Diagram shows that the studied sandstones are chiefly deposited by beach/tidal process. The log-probability weight percentage frequency curves suggest the erraticism (variability) of the hydraulic depositional conditions for the Bredasdorp Basin sandstones. The main mode of transportation is by saltation, followed by suspension and traction. Also, the log probability grain-distribution curves show that the sandstones were primarily affected by tidal flow and ebb currents during their transportation and deposition.

Generally, the depositional environments deduced from sedimentary facies analysis agree to an extent with those from grain size analysis. For example, the ripple cross-laminations in the Sr facies are usually traction features that result from bed-load transport during deposition by unidirectional currents (i.e., turbidity currents). These traction features perhaps suggest that FA 2 was deposited by turbidity flows that may have separated from medium-to high-density turbidity currents. Likewise, the alternation of mudrock and sandstone beds suggests that the deposition occurred under fluctuating energy conditions. Again, the alternation of laminated units with clay-rich units points to the fact that different kinds of low-density turbidity currents alternated within the water column. In support of the presence of fluctuating hydrodynamic conditions and the influence of the turbidity current, the grain size binary plot of the skewness against mean (Figure 8) shows that the samples plotted in the coastal and dune environments of [29] and [13]. Also, most of the samples clustered in the fields of wave and river processes of [37], with the wave processes dominating. This bivariate diagram shows an overlapping of plots, perhaps indicating a multiple influence of river, dune and beach environmental conditions. In addition, the linear discrimination functions (LDF) binary plots presented in Figure 11 show that the studied stratigraphic sequence of the Bredasdorp Basin is of shallow marine environment and turbidity current deposits (agitated water). The weakness in the grain size analysis is that it could not differentiate between shallow marine and deep marine sediments. The deduced depositional environments in this study are comparable to or support the depositional interpretation of the Bredasdorp Basin as reported by [21,23,27] using seismic analysis. According to McMillan *et al.* [27], during the rifting phase when half-graben basin styles were dominant, sediments accumulated in a wide range of environments (non-marine to slope). In the Bredasdorp Basin, where major bounding faults are less well developed, sediments were laid down in non-marine and marginal marine environments, resulting

in the widespread development of red and green claystones overlain by clean, porous glauconitic littoral sandstones.

## 6. Conclusions

Grain size and lithofacies analyses were combined and used to interpret the depositional environments of mudrocks, sandstones, and conglomerates in the southern Bredasdorp Basin's 6At1 and 14At1 stratigraphic sequences. The grain size distribution reveals that the sandstones of the Bredasdorp Basin are mostly fine-grained, moderately well-sorted, mesokurtic, and nearly symmetrical. The fine sand nature of the sediments indicates that a moderately low energy condition prevails in the study area. The well sorted to moderately well sorted nature of the sediments suggests an abrupt winnowing and back and forth movement by the depositing agents. The dominance of the near symmetrical category could be attributed to riverine input and mixing of similar modal fractions. The unimodal distribution of the sediments demonstrates the stable depositional process that laid down the Bredasdorp Basin sediments. The sediments are turbidity current deposits under coastal dune and beach processes in a shallow marine environment, according to the linear discriminant functions (LDF) analysis. The C-M pattern (Passega Diagram) indicates that the sediments in the Bredasdorp Basin were deposited primarily by rolling, rolling and suspension, suspension and rolling, and uniform suspension. Furthermore, the Passega Diagram demonstrates that the studied sandstones were deposited primarily by the beach process. The log-probability weight percentage frequency curves revealed that tidal flow and ebb currents were the primary influences on sediment deposition. A total of thirteen lithofacies were discovered and classified into six distinct facies associations (FAs). The sediments are shallow and deep marine deposits, according to sedimentological evidence from facies interpretation. Submarine channel, submarine channel-levee, submarine sheet lobe, and submarine lobe fringe deposits are represented by FA 1 (Gmm + Sm), FA 2 (Sr + Sh + Sb), FA 3 (Sm + Fmb + Fl), and FA 4 (Sl + Smp + Fl + Fsm). FA 5 (Fsm + Fmb + Fms + Sb + Sml) basin plain and FA 6 (Fc + Fl + Fms) deep sea floor/basin plain deposits, respectively. These environments reveal sedimentary characteristics deposited during several high frequency transgressive and regressive events ranging from the coastal area to the abyssal plain.

## References

- [1] Chima P, and Baiyegunhi C. Textural characteristics, mode of transportation and depositional environment of the Stormberg Group in the Eastern Cape, South Africa: evidence from grain size and lithofacies analyses, *Geologos*, 2022; 28: 61–78.
- [2] Middleton GV. Facies. [In:] R.W. Fairbridge & J. Bourgeois (Eds): *Encyclopaedia of sedimentology*. Dowden, Hutchinson & Ross, Stroudsburg, 1978; 323–325.
- [3] Reading HG. *Sedimentary environments processes, facies and stratigraphy*. 3rd Edition. Blackwell, 1996; 422–448.
- [4] Miall AD. *The Geology of Fluvial Deposits: Sedimentary Facies, Basin Analysis and Petroleum Geology*, Springer, New York, USA, 1996; 22p.
- [5] Nyathi N. *Stratigraphy, sedimentary facies and diagenesis of the Ecca Group, Karoo Supergroup in the Eastern Cape, South Africa*. MSc. dissertation (Unpublished), University of Fort Hare, South Africa, 2014; 142p.
- [6] Boggs S. *Principles of Sedimentology and Stratigraphy*, 4th -ed., Prentice Hall, Upper Saddle River, NJ. 2006; 774p.
- [7] Bui EN, Mazullo J, and Wilding, LP. Using quartz size and shape analysis to distinguish between aeolian and fluvial deposits in the Dllot Bosso of Niger (West Africa). *Earth Surface Processes and Landforms*, 1990; 14: 157–166.
- [8] Rao TCS, Machado XT, and Murthy KSR. Topographic features over the continental shelf off Visakhapatnam. *Mahasagar-Bulletin National Institute of Oceanography*, 2005; 13: 83–89.
- [9] Baiyegunhi C, Liu K, and Gwavava O. Grain size statistics and depositional pattern of the Ecca Group sandstones, Karoo Supergroup in the Eastern Cape Province, South Africa. *Open Geosciences*, 2017; 9: 554–576.
- [10] Folk RL. *Petrology of Sedimentary Rock* (second ed.), Hemphill Press, Austin, Texas, 1974; 182p.

- [11] Folk RL, and Ward W. Brazos river bar: a study in the significance of grain size parameters. *Journal of Sedimentary Petrology*, 1957; 27: 3–26.
- [12] Friedman GM. Differences in size distribution of populations of particles among sands of various origin, *Sedimentology*, 1979; 26: 859–862.
- [13] Moina RJ, and Weiser D. Textural parameters: an evaluation. *Journal of Sedimentary Petrology* 1968; 38: 45–53.
- [14] Duck RW. Applications of the QDa-Md method of environmental discrimination to particle size analyses of fine sediments by pipette and sedigraph methods: a comparative study. *Earth Surface Processes Landforms* 1994; 19: 525–529.
- [15] Passega R. Sediment sorting related to basin mobility and environment. *American Association of Petroleum Geologists* 1972; 56: 2440–2450.
- [16] Folk RL. A review of grain-size parameters. *Sedimentology* 1966; 6: 73–93.
- [17] Reid LM, and Dunne T. *Rapid Evaluation of Sediment Budgets*. Catena, Reiskirchen, 1996; 164 p.
- [18] Visher GS. Grain size distributions and depositional processes. *Journal of Sedimentary Petrology*, 1969; 39:1074–1106.
- [19] Sagoe KMO, and Visher GS. Population breaks in grain-size distributions of sand - a theoretical model. *J Sediment Petrol*, 1977; 47 (1): 285–310.
- [20] Sonibare WA. Structure and evolution of basin and petroleum systems within a transform-related passive margin setting: data-based insights from crust-scale 3D modelling of the Western Bredasdorp Basin, offshore South Africa. PhD. Thesis, University of Stellenbosch, 2015; 294p.
- [21] Brown LF, Benson JM, Brink GJ, Doherty S, Jollands A, Jungslager EHA, Keenan JHG, Muntingh A, and Van Wyk NJS. Sequence stratigraphy in offshore South African divergent basins. In: *Am. Ass. Petrol. Geol., Studies in Geology*, 41, *An Atlas on Exploration for Cretaceous Lowstand traps*, by Soeker (Pty) Ltd, 1995; 83–131.
- [22] Petroleum Agency South Africa, PASA. Petroleum exploration in South Africa, information and opportunities. Online Report, Cape Town, 2012; 25–29. [http://www.petroleumagen-cysa.com/images/pdfs/pet\\_expl\\_opp\\_2012fw.pdf](http://www.petroleumagen-cysa.com/images/pdfs/pet_expl_opp_2012fw.pdf)
- [23] Broad DS, Jungslager EHA, McLachlan IR, and Roux J. Offshore Mesozoic Basins. In: Johnson MR, Anhaeusser CR, and Thomas RJ. (Eds.). *The Geology of South Africa*. Geological Society of South Africa, Johannesburg/Council for Geoscience, Pretoria, 2006; 553–571.
- [24] Burden PLA, and Davies CPN Exploration to first production on block 9 off South Africa: *Oil and Gas Journal*, 1997; 1: 92–98.
- [25] Akinlua A, Sigidle A, Buthelezi T, and Fadipe OA. Trace element geochemistry of crude oils and condensates from South African Basins. *Marine and Petroleum Geology*, 2015; 59: 286–293.
- [26] Tinker J, de Wit M, and Brown R. Linking source and sink: evaluating the balance between onshore erosion and offshore sediment accumulation since Gondwana break-up, South Africa. *Tectonophysics*, 2008; 455 (1): 94–103.
- [27] McMillan IK, Brink GJ, Broad DS and Maier JJ. Late Mesozoic sedimentary basins off the south coast of South Africa, in Selley, R.C., ed., *Sedimentary basins of the world—African basins*: Amsterdam, Elsevier Science B.V., 1997; 319–376.
- [28] Jungslager EHA. Geological evaluation of the remaining prospectivity for oil and gas of the Pre-1At1 “Synrift” succession in Block 9, Republic of South Africa. Unpublished Soekor Technical Report SOE-EXP-RPT-0380, 1996; 63p.
- [29] Friedman GM. Distinction between dune, beach and river sands from their textural characteristics. *Journal of Sedimentary Petrology*, 1961; 31: 514–529.
- [30] Wentworth CK. Method of computing mechanical composition types in sediments. *Bull. Geol. Soc. Am.*, 1929; 40: 771–790.
- [31] Baiyegunhi C, and Liu K. Sedimentary facies, stratigraphy and depositional environments of the Ecqa Group, Karoo Supergroup in the Eastern Cape Province of South Africa. *Open Geosciences*, 2021; 13: 748–781.
- [32] Sahu BK. Depositional mechanism from the size analysis of elastic sediments. *Journal of Sedimentary Petrology*, 1964; 34 (1): 73–83.
- [33] Passega R. Grain size representation by C-M pattern as a geological tool. *Journal of Sedimentary Petrology* 1964; 34: 830–847.
- [34] Boggs S Jr. *Petrology of Sedimentary Rocks*, Second Edition. Cambridge University Press, UK, 2009; 600p.

- [35] Ramanathan AL, Rajkumar K, Majumdar J, Singh G, Behera PN, Santra SC, and Chidambaram S. Textural characteristics of the surface sediments of a tropical mangrove Sundarban ecosystem, India. *Indian Journ. Mar Sci.*, 2009; 38 (4): 397–403
- [36] Duane DB. Significance of skewness in recent sediments, western Pamlico Sound, North Carolina: *Journal of Sedimentary Petrology*, 1964; 34 (4): 864–874.
- [37] Stewart HB. Sedimentary reflection on depositional environment, in San Mignellagoon, Baja California, Mexico *AAPG Bull*, 1958; 42: 2567–2618.
- [38] Friedman GM. Dynamic processes and statistical parameters compared for size frequency distribution of beach and river sands. *Journal of Sedimentary Petrology*, 1967; 37: 327–354.
- [39] Passega R. Texture as characteristics of clastic deposition. *American Association of Petroleum Geologists Bulletin* 1957; 41: 1952–1984.
- [40] Pickering K, Stow D, Watson M, and Hiscott R. Deep-facies, processes and models: a review and classification scheme for modern and ancient sediments. *Earth-Sciences Review*, 1986; 23: 75–174.
- [41] Pemberton SG, MacEachern JA, and Frey RW. Trace fossil facies models: environmental and allostratigraphic significance. In Walker RG, and James N. (eds.), *Facies Models: Response to Sea Level Change*. Geological Association of Canada, 1992; 47-72.
- [42] Hocking RM. The Silurian Tumblagooda Sandstone, Western Australia. *Geol. Surv. W. Aust. Rep.*, 1991; 27: 124p.
- [43] Saito T, and Ito M. Deposition of sheet-like turbidite packets and migration of channel-over-bank systems on a sandy submarine fan: an example from the late Miocene-Early Pliocene fore arc basin, Boso Peninsula, Japan. *Sedimentary Geology*, 2002; 149: 265–277.
- [44] Habgood EL, Kenyon NH, Masson DG, Akhmetzhanov A, Weaver PPE, Gardner J, and Mulder T. Deep-water sediment waves fields, bottom current sand channels and gravity flow channel-lobe systems: Gulf of Cadiz, NE Atlantic. *Sedimentology*, 2003; 50: 483–510.
- [45] Megner-Allogo A. Sedimentology and Stratigraphy of deep-water reservoirs in the 9A to 14A Sequences of the central Bredasdorp Basin, offshore South Africa. MSc dissertation (Unpublished), Stellenbosch University, 2006; 203p.

---

*To whom correspondence should be addressed: Dr. Temitope Love Baiyegunhi, Department of Geology, Faculty of Science and Agriculture, University of Fort Hare, Private Bag X1314, Alice, 5700, Eastern Cape Province, South Africa, E-mail: 201814648@ufh.ac.za; lovetemitope18@gmail.com*